CONF-760317--2
DP-MS-74-39

STRUCTURAL AND SEDIMENTATIONAL MODEL OF THE BURIED DUNBARTON TRIASSIC BASIN, SOUTH CAROLINA AND GEORGIA

by

I. W. Marine

Savannah River Laboratory
E. I. du Pont de Nemours and Co.
Aiken, South Carolina 29801

For presentation at the *1976 Annual Meeting of the Geological Society of America Southeastern Section* in Arlington, Virginia, March 25-26, 1976, and for publication in *Geological Society of America Bulletin*.

This paper was prepared in connection with work under Contract No. AT(07-2)-1 with the U. S. Energy Research and Development Administration.

DISCLAIMER

STRUCTURAL AND SEDIMENTATIONAL MODEL OF THE BURIED DUNBARTON TRIASSIC BASIN, SOUTH CAROLINA AND GEORGIA*

by

I. W. Marine

Savannah River Laboratory
E. I. du Pont de Nemours and Co.
Aiken, South Carolina 29801

ABSTRACT

The Dunbarton basin is located on the South Carolina-Georgia boundary about 32 km southeast of the Fall Line. It consists of red mudstone and sandstone of Triassic age and is buried beneath 350 m of unconsolidated Coastal Plain sediments. Seismic reflection surveys and model interpretation of gravity-magnetic surveys indicated that the Dunbarton basin may consist of fault blocks of different thicknesses with displacements of <30 m on the top of the Triassic rock and 92-760 m on the bottom. Drilling showed that the apparent displacement on the top was caused by the presence or absence of a reflector in the Coastal Plain sediments that masked the reflection from the top of the Triassic rock. No fault displacement has occurred since the development of the erosional surface on the top of the Triassic rock about 100 million

* The information contained in this article was developed during the course of work under Contract No. AT(07-2)-1 with the U. S. Energy Research and Development Administration.

years ago. Drilling information did not confirm or deny the displacement of the bottom of the Triassic basin. Model interpretation of the gravity-magnetic data indicates that the Dunbarton Triassic basin may be wider than previously interpreted, and is in part underlain by a denser basement rock, possibly a pre-Triassic igneous intrusion.

Prior to the intrabasinal faulting, when the Triassic sediments were filling the basin, a mountainous highland existed to the northwest that was separated from the basin by a border fault similar to those in the Basin and Range province today. The metamorphic rock presently found beneath the Coastal Plain sediments in this region of Triassic highlands accounts for all of the lithologic types of fragmental rocks found in the Triassic basin. Mudrock flow material moved from the mountain face in the interstream areas of the Triassic basin and these poorly sorted deposits of mud and boulders are penetrated by a well near the northwest edge of the basin. Farther from the mountain face, deposits of the same poorly sorted sediments occur but without boulders or material generally coarser than granule size; these deposits are penetrated by a well about 2¼ km from the northwest edge of the basin. Streams that drained the mountainous region back from the face deposited alluvial fans that enlarged areally but decreased in grain size as distance from the mountains increased. These muddy sand deposits are penetrated by a well about 6 km from the northwest edge of the basin. Based on the

mineralogy of the sediments at these last two wells, subsequent erosion not only removed the Triassic highland, but also removed 1800 to 2400 meters of Triassic sediments.

INTRODUCTION

The Dunbarton Triassic basin is located on the South Carolina-Georgia boundary about 32 km southeast of the Fall Line (Fig. 1). The basin is buried beneath about 350 m of unconsolidated Coastal Plain sediments and is perhaps 1620 m thick at its deepest point. The Triassic rock consists of maroon mudstone and poorly sorted sandstone and conglomerate. Because the basin is completely buried by the Coastal Plain sediments, study is restricted to geophysical investigations and exploration wells. The basin was discovered by an exploration well in 1962. Subsequently, a small amount of geophysical work was done, and two additional exploration wells were drilled. The results of these studies are reported by Marine and Siple (1974).

Because the Dunbarton Triassic basin was considered to have potential for a mined facility for storage of radioactive waste at the Energy Research and Development Administration's Savannah River Plant (SRP), exploration was intensified in 1971. However, in 1972 it was indefinitely postponed before the planned program was completed, in order to examine alternative methods of waste disposal. Exploration that started in 1971 included about 129 km of seismic reflection traverse, 140 km of gravity-magnetic traverse, and the drilling of two additional exploration wells.

The results of these investigations suggest an alternate concept of the shape and size of the basin to the one given by Marine and Siple (1974). The results also provide additional information on the nature and age of faulting within the basin and on the possible character of the underlying rocks. Studies of the lithology and mineralogy of cores of the two wells also permit the development of a sedimentational model.

The structural and sedimentational models of this subsurface Triassic basin provided by the additional geophysical exploration and exploratory drilling are the subjects of this report.

PREVIOUS CONCEPT OF THE DUNBARTON TRIASSIC BASIN

The concept of the Dunbarton Triassic basin presented by Marine and Siple (1974) is that of a basin ~50 km long and 10 km wide, elongated in a northeasterly direction. The northwest margin was well located and appeared to be a sedimentary contact dipping 35° to the southeast. A border fault is nearby but because of post-Triassic erosion, the fault is now wholly located within the crystalline metamorphic rock (Fig. 2). Mudrock flow deposits are the predominant sediments near the northwest margin of the basin. Farther southeast toward the center of the basin the sediment becomes sandstone and mudstone.

Much less information is available on the southeast margin of the basin, but an abrupt increase in the magnetic field intensity (indicated on the aeromagnetic map in Fig. 3), was interpreted as a border fault of large displacement (Fig. 2).

A nearby well (P5R, Fig. 2 and 3) penetrated only mudstone and fine-grained sandstone in 29 m of Triassic rock. Conglomerates would be expected at this location if a southeastern border fault occurred during sedimentation as did the northwestern fault.

Similar discrepancies between sediment size and the proximity of a large border fault have been noted in other exposed Triassic basins (Randazzo et al., 1970), which are referred to as half-grabens. The explanation offered by Randazzo et al. (1970) is that subsequent to the formation of a symmetrical basin with faults and conglomerates on both sides, the basin has been split in half by a major fault with only the downthrown block preserved. However, the half-graben nature of the Dunbarton Triassic basin is not observed; rather, it is inferred primarily from one well and a simplistic interpretation of the magnetic field intensity contours as reflecting the depth to the crystalline metamorphic rock. Additional information reported here casts some doubt on this interpretation of the aeromagnetic map and on the abrupt termination of the Triassic sediments by a southeastern border fault as shown in Figure 2.

Prior to the completion of the seismic studies reported herein, the only information on the upper surface of the Triassic basin was that it was (1) of low relief, (2) correlative with the erosion surface on the crystalline metamorphic rock to the northwest (Fig. 2) which was also of low relief, and (3) that it sloped

at about the same angle as the surface of the crystalline metamorphic rock. All of these items of information arise from the fact that very accurate predictions had been made of the depth to the top of the Triassic basin in two wells by planar extrapolation of the surface of the crystalline metamorphic rock which was known in greater detail (wells in northwest part of SRP as shown on Fig. 3).

The seismic reflection studies of this investigation indicated that the upper surface of the Triassic basin might be cut by several faults with displacements of less than 30 m; however, two exploration wells, one on either side of one of these inferred faults, demonstrated conclusively that there was no displacement of the Triassic basin surface. Even though only one seismically inferred fault was investigated by drilling, the results cast doubt on the validity of the other inferred faults.

The only information available prior to the present study on the contact of Triassic rock with underlying rock was obtained from an exploration well located less than a kilometer southeast of the northwest edge of the basin where a well (DRB 9, Fig. 3) penetrated an augen-gneiss after passing through 485.5 m of Triassic rock. The northwest margin of the basin is inferred to dip 35°. If this dip were projected to the location of the southeast margin interpreted by Marine and Siple (1974), the Triassic basin there would be 7 km thick. This great thickness seems unlikely for such a narrow basin, but no information on

its thickness was available until the present studies were made. Conceptual models based on gravity and magnetic surveys indicate that the basin is not a simple wedge thickening to the southeast but consists of several blocks of unequal thicknesses. In addition, these conceptual models indicate that the rock beneath the Triassic basin changes from chlorite-hornblende schist or augen-gneiss to a rock of greater density and higher magnetic susceptibility, possibly a gabbro or an intrusive rock of similar density and magnetic properties.

Information on the character of the Triassic rock itself was previously derived from core samples from three wells. The two additional wells that were drilled do not alter any previous concepts (Marine and Siple, 1974) of the character of the rock, although they permit a refinement in the sedimentational model of the basin. No igneous rocks or coal beds have been found within the Dunbarton Triassic basin.

STRUCTURAL MODEL

Additional Geophysical and Geological Exploration

The purpose of the additional geophysical exploration was to map the upper and lower contacts of the Triassic rock, thereby determining the shape and size of the Triassic basin, and to determine whether faults existed. These geophysical studies included 129 km of continuous seismic reflection traverse (Fig. 4) with 275 m between shot points and 140 km of gravity and magnetic traverses (Fig. 3 and 4) with stations approximately 400 m apart. The seismic traverses and the basic geophysical inter-

pretation were made by a seismic exploration contractor and the gravity and magnetic surveys and their basic geophysical interpretation were made by a gravity-and-magnetic exploration contractor.

The contact of the Triassic basin with the crystalline metamorphic rock below could not be detected on any of the seismic traverses. As reported by Marine (1974), the seismic wave velocities increase with depth and approach the wave velocities in crystalline metamorphic rock near the bottom of the basin, thus giving low seismic contrast between the two varieties of rock.

Although an occasional reflecting layer was apparent within the Triassic rock, these could not be correlated consistently to indicate any extensive bedding.

The seismic reflection at the contact between the Coastal Plain sediments and Triassic rock generally showed good correlation; however, in several disturbed zones possible minor faulting was indicated. These zones of inferred possible faulting are shown on Figure 4, and one of the more probable of these zones was selected for further exploration by drilling two exploration wells (DRB 11 and P12R, Fig. 4), one on the upthrown and one on the downthrown side of this inferred fault.

The gravity and magnetic surveys provide profiles of the change in the acceleration of gravity and in the vertical magnetic field intensity. The methods of interpretation involve constructing models that would theoretically duplicate the observed profiles. There may be several acceptable models, but when the known

information from drill holes and from seismic exploration are incorporated, the models tend to become more unique. Thus, these methods achieve their greatest utility in the areal extrapolation of knowledge gained by other means and in guiding an exploration program. Unfortunately, several key items of information for interpreting these profiles were not obtained, but the interpretive models that were developed are useful in the overall conceptual model of the Dunbarton Triassic basin. Because the density and magnetic properties of the Triassic rock are similar to those of the Coastal Plain sediments (density = 2.43), it was assumed that the gravity and magnetic profiles do not "see" the top of the Triassic basin. However, the density contrast between the underlying crystalline metamorphic rock (density = 2.73) and these shallower sedimentary rocks is such that all characteristics of the profiles are attributed to changes in either the depth or character of the metamorphic rocks.

The gravity and magnetic interpretive models indicated displacements of the crystalline metamorphic rock in the same locations where the seismic profiles indicated displacement of the surface of Triassic rocks (Fig. 5) and in a few additional locations. So the modeling results of the gravity and magnetic surveys, performed after the seismic results were available, reinforced the existence and location of the faults inferred from seismic reflection measurements.

To develop more positive information on the existence, location, and geohydrologic character of the inferred faults, one was selected for exploration, and an exploratory well was located on either side of the inferred fault. Both of these wells were to be deviated from the vertical toward the inferred location of the fault and toward each other. After completion, these two wells would have explored all geometrical possibilities for the dip and attitude of the inferred fault plane. To assure that the fault, if it existed, was not missed by the wells, continuous core was taken from the Triassic section of both wells. Because the program was not completed, only one of these wells was drilled to its planned depth. The other well (P12R), which was drilled first, penetrated only a short distance into the Triassic basin to establish the location of its top. The intention was to return to this hole if the inferred fault was not penetrated by the second hole (DRB 11).

Shape and Size of the Basin

The previous interpretation (Marine and Siple, 1974) of the shape and size of the Dunbarton Triassic basin was based almost entirely on a consideration of a closed depression in the aeromagnetic contours as shown on Figure 3. This interpretation was reinforced by the seismic and drilling exploration of the northwest margin of the basin. The additional seismic work reported herein indicates general agreement with this outline (Fig. 3) except that there is no definite change in the character of the reflection

where it was interpreted that the crystalline metamorphic rock should underlie the Coastal Plain sediments at the southeast border of the basin. The seismic traverse extended 8 km southeast of what had been interpreted as the southeast margin of the basin. Even though there were several inferred faults in this area (Fig. 4), none of these was clearly the border fault that terminated the top of Triassic reflection.

Termination of the Dunbarton Triassic basin on the southeast is not required for a model based on gravity and magnetic profiles (Fig. 5). To locate the southeastern termination of the Triassic rock, a gravity-magnetic profile was extended to Barton, South Carolina, about 34 km southeast of the SRP boundary (Fig. 3). Barton is about 3 km southeast of a change in aeromagnetic characteristics (Fig. 3) from discontinuous highs and lows of great magnitude that are characteristic of the area southeast of the previously interpreted Triassic border to a broad area of little magnetic relief. Thus, any interpretation of this data relative to the Triassic basin to the southeast of Barton becomes much more tenuous.

Both the seismic interpretation and the models based on gravity and magnetic data are tenuous and only indicate the possibility that the Dunbarton Triassic basin is wider than 10 km. From drilling information it is known that lenticular reflecting horizons in the Coastal Plain sediments can mask the top of the Triassic rock reflector and could obscure its termination. The

gravity-magnetic models are greatly dependent on the assumed density and magnetic properties of the underlying rock. There are no well data on the basement rock southeast of the northwest margin of the basin to establish this density.

Upper Contact and Overlying Rock

The seismic reflection study northwest of the Dunbarton Triassic basin (Fig. 4) showed two clearly defined reflections as reported by Marine and Siple (1974). The lower of these correlates with the top of hard crystalline metamorphic rock. This reflection terminates at the northwest boundary of the basin. The upper reflection is known to be above the top of the saprolite (in-place weathered crystalline rock) and therefore is within the Coastal Plain sediments. In Well DRB 8 (Fig. 4), this reflection is 11.9 m above the top of the saprolite. This reflecting horizon can be followed continuously without a break across the northwest boundary of the basin. However, at the inferred fault shown between Wells DRB 11 and P12R on Figure 4, this reflection (labeled "Masking Reflector" on Fig. 6) terminates abruptly. It is replaced on the southeast side of the inferred fault by a reflection 29.0 m deeper (labeled "Top of Triassic Reflector" on Fig. 6). During early work it was appeared that these two reflectors were the same, and a fault was indicated with downthrow on the southeast. After the correlation of the rock in Well DRB 10 with the seismic work, it was realized that the reflectors on either side of the fault were different, and that if the top of the basin on the northwest

side of the inferred fault were uniformly 41.5 m below the masking reflector, as it is at Well DRB 9, the fault would be downthrown on the northwest (Fig. 4 and 6).

In view of the tenuous extrapolation of the 41.5-m interval for 2225 m on the northwest side of the fault, a hole was drilled on each side of the inferred fault (Wells DRB 11 and P12R, Fig. 4 and 6). The wells were drilled initially to casing-setting depth (45-60 m below the top of the Triassic rock) in order to obtain positive information on the displacement. Gravity and magnetic surveys indicated that the fault dipped steeply to the southeast, so the hole on the southeast side of the fault (Well DRB 11) would be the more likely to intersect the inferred fault.

The northwest well, P12R, was drilled first and coring began at an elevation of 210.6 m below sea level. The first core was lost, but at an elevation of -215.2 m a clayey sand that was hard, gray, gritty, and in some places gravelly, was encountered. This sand was probably the seismic reflector interpreted to be at an elevation of -213.6 m (Fig. 6). The top of the Triassic rock was encountered at an elevation of -242.3 m.

The hole on the south side of the fault (Well DRB 11) penetrated the top of the Triassic rock at an elevation of -242.9 m, confirming the extrapolation from Well DRB 10 of the seismic reflector that was interpreted to be the top of the Triassic rock.

Characteristics of core samples from these two wells, which are about 210.3 m apart, indicate that there is no significant displacement of the Triassic surface.

Absence of displacement on the Triassic rock surface means that there has been no movement on the inferred fault since the development of the erosion surface that forms the top of the crystalline and Triassic rock. Because this erosion surface developed between 100 million and 180 million years ago, the last movement on the fault, if it exists, was at least 100 million years ago, and it has not moved as a result of more recent tectonics of the Atlantic Coastal Plain.

Geophysical logs further corroborate the conclusion that the inferred fault has not moved since the deposition of the Cretaceous and Tertiary Coastal Plain sediments. The most useful logs for this purpose are those based on electric and gamma ray measurements. Correlation could be made of 12 distinctive points from the electric logs and 11 points from the gamma logs, ranging in depth from 57.3 to 326.0 m. With adjustments for a regional dip of 1.5 m between the two holes, these correlations indicate a south-side displacement ranging between a 2.1-m upthrow and a 1.8-m downthrow. The average indicates that the south side is upthrown by 0.3 m, and the median indicates that the south side is upthrown by 0.6 m. Uncertainties in the measurements of the two geophysical logs are such that these differences are not significant, and that there may be no measurable displacements in the vicinity of the inferred fault.

Thus, the seismically inferred fault is caused solely by the presence or absence of the masking reflector (Fig. 6). Even though the level of the masking reflector is occupied by gritty sand and small gravel in Well P12R, gritty sand and small gravel are common sediment types in the lower Coastal Plain sediments. Thus, the masking reflector must be caused by a more unique property than the presence of sand and gravel.

In the area where the Coastal Plain sediments are underlain by crystalline metamorphic rock, a gray silty clay directly overlies the saprolite. But overlying the Triassic rock is a unit consisting of coarse sand, grit, and even gravel, embedded within a sandy clay. This unit was noted by Marine and Siple (1974) and the suggestion was made that it may represent a unit different from the upper Cretaceous Tuscaloosa Formation.

Both of these units (the silty clay over the metamorphic rock and the gritty clay over the Triassic rock) are of low permeability especially when compared with the aquifer section of the Tuscaloosa. They are indicated on the electric log by a decrease in resistivity. At the contact with the Triassic rock the resistivity of the gritty, sandy-clay unit and that of the Triassic rock are nearly the same making the contact indiscernible on the electric log.

The sandy-clay unit with embedded grit and gravel exists on both sides of the inferred fault raising the question of why there was no reflection above the top of the Triassic rock on

the southeast side of the inferred fault. The available cores were examined to determine what similarities might exist at the masking reflector on the northwest and at the top of the Triassic rock on the southeast. The only common observation was that at each horizon there appeared to be some evidence of an ancient soil horizon. This took the form of a light-grayish clay (patches in the red Triassic rock) in which there was a much darker anastomosing pattern of dark gray clay giving the appearance of rootlets, although without any lignite preserved. Although this was a common property at the two reflecting horizons, these possible soil zones did not appear to be more dense than material above or below.

The other faults inferred from the seismic data shown on Figure 4 also were initially based on the displacement of the Triassic rock surface. These may also be caused by the lensing of the masking reflector across the seismic line.

Lower Contact and Underlying Rock

Well DRB 9, which is about 0.65 km from the northwest edge of the Dunbarton Triassic basin, passed through 485.5 m of Triassic rock and penetrated 20.4 m of augen-gneiss below (Marine and Siple, 1974). No other well has penetrated the rock underlying the Dunbarton basin. Therefore, at the location of Well DRB 10 (Fig. 4), the Triassic rock is greater than 925 m thick and at Well DRB 11 the rock is greater than 670 m thick. No seismic

reflection was observable from the lower contact of the Triassic rock, presumably because of the low velocity contrast. As a result of these facts, all of the information about the lower contact is derived from model interpretation of the gravity and magnetic data. A cross section of one of these models is shown in Figure 5.

The modeling of the gravity-magnetic data supported the location of a fault at each location indicated by the seismic work. In addition, the model required several other displacements not indicated by the seismic work. Displacements of the lower Triassic basin contact along these inferred faults were 92 to 760 m. Thus, the Dunbarton basin appears to consist of block-like units of different thicknesses separated by steeply dipping faults rather than a uniformly thickening wedge bounded by large displacement faults.

From its margin near Well DRB 9, the Dunbarton basin generally becomes deeper to a point about 3.5 km southeast of Well DRB 10 (cross section A-A', Fig. 3 and 5), where its depth is estimated to be about 2000 m. From that point, it shallows to about 1300 m at the southeastern boundary of SRP. Southeast of SRP (cross section A-A', Fig. 3 and 5), depths range from about 900 to 1800 m. These depths include the Coastal Plain sediments, which are similar to the Triassic rocks in their densities and magnetic properties. Thus, at Well DRB 10, according to this model, the Triassic rock would be about 1600 m thick, and at the southeastern boundary of SRP, thickness is about 900 m.

The gravity data also suggest a change in basement rock density about 760 m south of Well DRB 10 (Fig. 5), in order to avoid an outcrop of crystalline rock at SRP's southeastern boundary in the model. This denser rock has not been sampled, but the model shown on Figure 5 uses an assumed density of 3.17, an approximate average for ferromagnesian igneous rocks like basalt or gabbro. A density could have been assumed that would have resulted in the termination of the Triassic basin as originally interpreted from the aeromagnetic map. To verify any of these models, the density and magnetic properties of the underlying rock must be known, not assumed.

An idea of the outline of the denser body of underlying rock, irrespective of its absolute density, can be inferred if data from other gravity-magnetic traverses are used. These additional traverses show that the change in basement rock density should not be extrapolated along the strike of the axis of the Triassic basin or along the strike of the schistosity of the crystalline metamorphic rock. The mass of denser basement rock appears to be irregular or subcircular in outline as indicated in Figure 4. The denser underlying rock may be an igneous intrusion, as many igneous intrusions in the Piedmont of South Carolina are subcircular in outline.

Intrabasinal Faulting

As explained in the subsection "Upper Contact and Overlying Rock," seismic indication of fault displacement of the surface

of the Triassic rock was shown to be spurious and due to the lensing of the masking reflector in the Coastal Plain sediments. However, the model interpretation of the gravity and magnetic data indicated displacements on the lower Triassic contact, even if these inferred faults had not moved since the development of the Triassic basin surface. Wells DRB 11 and P12R were drilled primarily for the purpose of investigating the model interpretation of the fault and, if a fault was present, to determine its geologic and hydrologic characteristics.

Well DRB 11 was designed to deviate 15° from vertical to intercept the fault that had been indicated by the gravity-magnetic surveys (Fig. 7). The deviation was obtained by periodically placing a 1.5°-steel wedge in the bottom of the hole and coring a smaller pilot hole with the 1 to 1.5°-deviation 4.6 m beyond the wedge, then removing the wedge, reaming the pilot hole to full size, and extending this deviant coring 15.2 m. The wedge was actually used 17 times, and the hole reached an inclination of 14° between the measured hole lengths of 392.2 and 639.3 m. Between measured hole lengths of 636.3 and 914.7 m, the wedge was used 5 times to hold the inclination between 13 and 14°. From measured hole lengths of 914.7 m to the end of the hole at 1012.6 m, the angle was allowed to decrease to a final 11.5° from vertical.

Well DRB 11 is shown in Figures 7 and 8. True vertical depth is 999.8 m; horizontal displacement between top and bottom

is 118.0 m northwest; the bottom is 17.4 m beyond the expected midplane of the indicated fault zone by seismic and gravity-magnetic measurements, but is 32.9 m short of the far boundary of the zone.

Two zones of the well are noteworthy; both are shown in Figure 7. In the "caving zone" from measured hole lengths of 712.8 to 714.3 m, numerous fractures were present and occasionally broken pieces of rock (2.5 to 5.0 cm) caved into the hole. This zone had numerous interlacing fractures, but slickensides were not generally present. No fault gouge was found. This caving zone appeared not to be a fault.

The second noteworthy zone is the sheared zone between measured hole lengths of 990.6 and 992.1 m, where numerous breaks were found in the core, all of which had slickensides. This zone was 15 m past the inferred fault zone midplane. In addition, the bottom of this zone contained 2.5 to 3.8 cm of gouge material of 0.6 cm and finer size. These two features indicated that displacement had occurred along this zone.

Because this sheared zone occurs in mudstone, which can exhibit these features with very little movement and because the rock type is identical on both sides, neither the amount of movement nor regional significance of any apparent movement can be estimated. The location of the sheared zone is consistent with that indicated by the gravity and magnetic surveys, and it was the only zone showing movement penetrated by Well DRB 11.

However, the dip of the zone of gouge material was only about 20°, whereas the dip of the fault inferred from the magnetic model was 80-90°. Thus, this sheared zone is probably not the major fault that was sought.

Because Well P12R was not completed, no definite statement can be made as to whether the fault inferred from gravity-magnetic data was present or not.

SEDIMENTATIONAL MODEL

Lithology of Sediments in the Dunbarton Basin

Descriptions and photographs of the Triassic sediments penetrated by Wells P5R, DRB 9, and DRB 10 (Fig. 3), are given by Marine and Siple (1974). Generally the sediments at Well P5R, near the possible axis of the basin and perhaps near the southeastern border, were maroon claystone and siltstone containing gray calcareous nodules, and grayish-brown sandstone that was fine to very fine-grained. The calcareous nodules were interpreted to be caliche.

The sediments at Well DRB 9, near the northwestern border of the basin, consisted of rock fragments of schist, gneiss, and quartzite, which ranged in size from granules to boulders, embedded in a maroon siltstone matrix. Much of the sediment apparently originated as mudrock flows from the nearby steep fault scarp that formed the northwestern edge of the basin. There was no calcareous material either as nodules or as cement in Well DRB 9.

There were three types of rock represented at Well DRB 10, located near the possible axis of the basin. These rocks were (1) maroon mudstone including clay, silt, and some fine-grained sand, (2) grayish-brown, fine- to medium-grained sandstone including much silt and clay, a graywacke, and (3) a pink to buff, medium- to coarse-grained arkosic sandstone. Sporadically, grit and small pebbles occur as well as clasts of the maroon mudstone similar to the mudstone at other depths in the well. Calcareous cement occurs commonly but not universally throughout the rock from Well DRB 10. Based on the composition of the core, which represented 10 percent of the rock penetrated by Well DRB 10, and on the geophysical logs, about 60 percent of the sediments were sandstone and about 40 percent were mudstone. Cross bedding occurs in some of the sand, and the depositional environment was apparently fluvial.

Well DRB 11 is 2225 m southeast of Well DRB 9 and 3810 m northwest of Well DRB 10 (Fig. 4). One reason for drilling the well in this location (the other reason being to explore an inferred fault) was to determine the relationship of the mudrock flow deposits at Well DRB 9 to the fluvial sands and muds at Well DRB 10. The Triassic section of Well DRB 11 was completely cored and core recovery was 100 percent. The dominant sediment making up 90 percent of the core was maroon, fine-grained mudstone. The remaining 10 percent consisted of widely interspersed layers

of gravel and coarse sand embedded in a mud matrix. Green spots, green patches, and thin green layers are interspersed in the predominantly red mudstone. Although the core commonly splits along these layers, there generally was no difference in grain size at these layers except for occasional green layers containing clay. Apparently the green patches represent local reducing conditions in an otherwise oxidizing environment.

Bedding is essentially absent from Well DRB 11 except for the overall layers of coarse material. The most likely environment of deposition is that of mudflows with only an occasional supply of coarse material. The sediments appear to be more closely related to those of Well DRB 9 than to those of Well DRB 10, in that both the muds and coarser materials are similar in character but are different in size and amount. In contrast to this, sediments like the pink arkosic sandstone or the gray sandstone in Well DRB 10 are rare at Well DRB 11.

The sediments at Well P12R are very similar to those at Well DRB 11, which is not surprising because this well is only 210 m northwest of Well DRB 11.

Mineralogy of the Sediments of the Dunbarton Basin

Mineralogic analyses of samples from the exploration wells were used to reconstruct the source region and to infer the depositional and diagenetic history of the basin.

The mineralogy of core samples from Well DRB 10 as determined by x-ray analysis by the U. S. Geological Survey (USGS) is given

in Table 1. Mineralogic analysis of samples from Well DRB 10 was also done by thin section petrography and is given in Table 2. In general, the thin section petrography provides a larger value for the percent of quartz and is thought to provide the more reliable value for this constituent. However, the x-ray analysis provides information on the clay minerals that is not available from the thin section analysis.

Mineralogy of samples from Well DRB 11 determined by x-ray techniques at the Savannah River Laboratory are given in Table 3. Further x-ray analyses were done on only the clay fraction (<2 microns) of 5 samples from Well DRB 11, and these results are given in Table 4. The mineralogy of samples from Well P12R were analyzed by x-ray diffraction, and these results are given in Table 5.

The cores of Wells DRB 10, DRB 11, and P12R can be divided into three distinct zones on the basis of mineralogy (Tables 1, 3, and 5). The upper zone consists of post-Triassic sediments, the middle zone is weathered Triassic rock near its erosional surface, and the lower zone is unweathered Triassic rock.

Each of the three groups can be distinguished readily from the other two. The upper zone (Coastal Plain sediments) is different from the lower because the upper is higher in quartz, potassium feldspar (orthoclase), and kaolinite contents; plagioclase is not present. The upper zone is different from the middle zone because the upper contains more quartz and potassium

feldspar, and less kaolinite. The middle zone differs from the lower zone in that it contains no potassium feldspar, but contains less plagioclase feldspar and more kaolinite. The middle zone is possibly a soil; hence, its low feldspar and high kaolinite are probably due to chemical change by previous circulation of ground water. In the lower zone (unweathered Triassic rock), mineral abundances are: potassium feldspar consistent a few percent, plagioclase a few tens of percent, chloride several percent, and kaolinite is nonexistent. Illite is the most common clay mineral in unweathered Triassic rock, and only a trace of montmorillonite was found.

The lack of kaolinite everywhere in the Triassic basin except in the top section conforms to the following postulated clay mineral reactions (Pettijohn, Potter, and Siever, 1972).

Some Clay Mineral Reactions During Sandstone Rock Formation (Diagenesis)

Clay Mineral Formed	*Precursor*
Kaolinite	Feldspar
Kaolinite	Pore Space
Illite	Kaolinite
Muscovite	Kaolinite
Illite	Montmorillonite
Chlorite	Montmorillonite
Montmorillonite	Volcanic Glass
Glauconite	Illite

Kaolinite is changed to illite at depth. Montmorillonite also changes to illite at depth. USGS x-ray data from Well DRB 10 samples indicate that the majority of montmorillonite found in Well DRB 10 was near the top. The cores from the top of both

Wells DRB 10 and P12R swelled and cracked, which was probably caused by exposure of the montmorillonite to fresh water from the atmosphere.

No mineralogic differences were seen between core that cracked when dried and core that did not; however, montmorillonite could not be identified on the x-ray machine used for the analysis of the samples from Well P12R, and this mineral may have been responsible for the cracking.

No mineralogic difference was found between green spots and the surrounding maroon mudstone, except for the presence of hematite. A possible explanation for this is the formation of humic acid by decaying organic material in a localized region, giving rise to reducing conditions that would prevent the oxidation of ferrous iron released from the hornblende.

Table 6 compares the average mineral composition of Well DRB 11 with that of the three rock types in Well DRB 10 and to the rock penetrated by Well P12R for those minerals that are not zoned vertically; that is, excluding the upper weathered layer of Triassic rock. The quartz content of the mudstones from Wells DRB 11 and P12R determined by x-ray analysis are higher (~55%) than that of the mudstone or sandstone from Well DRB 10 determined by x-ray analysis (~20%) but about the same as that determined by thin section analysis (~42%), as shown in Table 6. The quartz content of the crystalline schist and gneiss to the northwest, the probable source area for these sediments, is about 30%. The

quartz percentage ordinarily increases with transport when other minerals decay and are removed. Thus, the values for quartz content from thin section analysis are judged to be more reliable.

Samples from Well DRB 10 were analyzed for carbonate content, and the results are shown in the calcite column in Table 2. Carbonate is absent from large sections of the well, but a small percent is present in certain zones. Well DRB 11 penetrated a few zones with some calcite nodules, but in general calcite was more abundant in Well DRB 10 than in Well DRB 11.

Clay Mineralogy of the Dunbarton Basin

Because the trace of montmorillonite is difficult to identify when it is interlayered with illite, more refined mineralogic analyses were made on the clay minerals from five vertically distributed samples of mudstone from Well DRB 11 (Table 4).

The samples were taken from Well DRB 11 at depths of 331.9, 404.2, 480.1, 558.8, and 631.6 m. The sample taken at 331.9 m was only 5.5 m below the top of the Triassic rock. All samples were of such low permeability that any drilling mud (source of montmorillonite), which might have contaminated the samples, was limited to a very thin outer portion of the core. Material used for analysis was selected from the inner portion of the core.

All samples were first disaggregated into sand-size particles, then dispersed using a 2% solution of sodium carbonate. The <2-micron fraction was separated by centrifuge. Each sample was

chemically treated to enhance certain properties to allow more definitive x-ray identification of the clay minerals.

Perry and Hower (1972) postulated four stages of dehydration of argillaceous sediments containing montmorillonite. Stage 1 involves the loss of interstitial water and any interlayer water above two layers thick to the increasing pressure from overlying sediments. This initial compaction occurs within the first few hundred meters and is not considered as a diagenetic process. Stage 2 starts between depths of 1800 and 2400 m on the Gulf Coast and is the beginning of the diagenetic process. Here, some montmorillonite layers begin to be converted to illite layers. Stage 2 ends when approximately 65% of the montmorillonite layers have dehydrated and converted to illite layers. The onset of Stage 3 is recognized by the change from random to regular interlayering. During Stage 3, 80% of the montmorillonite layers become dehydrated. A hypothetical stage, Stage 4, is inferred but not actually seen in any wells. In this last stage, all of the montmorillonite should convert to illite. The exact depth at which conversions take place is dependent upon the geothermal gradient.

Table 4 lists the relative percentages of minerals in each sample. The general mineralogy of all five samples is similar and is dominated by illite-montmorillonite with lesser amounts of discrete illite, hematite, chlorite, and halloysite.

The results of further analyses on the illite-montmorillonite, mixed-layer material indicate a change from 12% illite layers to 38% within 305 m. These results would indicate that the top sample in the well has already reached Stage 2. The bottom sample, containing 38% illite layers, is also within the limits of Stage 2. Sediments that should have been nearly 100% montmorillonite above these are not present; presumably, they have been eroded away. These eroded sediments would comprise approximately 1800 to 2400 m of material if the geothermal gradient in Well DRB 11 (14.7°C/km, Marine, 1974) were comparable to that for the wells studied (24 to 31°C/km) on the Gulf Coast.

Source of Triassic Sedimentary Rock

The source region of the sedimentary Triassic rocks was inferred from (1) visual estimates of minerals and rock fragments from Wells DRB 9, DRB 10, and DRB 11; (2) x-ray data on Wells DRB 10, DRB 11, and P12R; and (3) comparison of these with data on basement crystalline rock below the plantsite (Christl, 1964).

From this evaluation, we conclude that a topographical high existed less than 24 km northwest of the basin during late Triassic time. This high region consisted for the most part of schists rich in hornblende, biotite, and chlorite, and of gneisses interspersed with macaceous quartzite lenses. A body of coarse-grained augen-gneiss also constituted a part of this high region but did not contribute as much coarse sediment as the schists and other gneisses. The body of augen-gneiss was probably of only local

extent. The other rocks are typical of the Carolina Slate Belt and extend over relatively large regions.

One major factor in determining the source region was the maturity (weathering) of the sediments. The Triassic rocks beneath the SRP site exhibit a very low degree of maturity as evidenced by the large size of rock fragments, the abundance of rock fragments and unweathered material, poor sorting, and sub-angular shape of the grains. Because maturity is "the measure of the approach of a clastic sediment to the stable end type to which it is driven by the formative processes operating on it" (Pettijohn, 1957), the maturity is also a combined record of the time through which such processes have operated and the intensities of their actions. Under conditions of rapid erosion, the chemical weathering processes are slower than the process of transportation; hence, much incompletely weathered material finds its way into the streams. Wells DRB 9, DRB 10, and DRB 11 all have an abundance of unweathered material. Of special note are the feldspars, usually one of the first minerals in a rock to be weathered. The average content of feldspar is 23 to 30 percent for all rock types in Wells DRB 10, DRB 11, and P12R (Table 6). The quartz-to-feldspar ratio is 2.4 in Well DRB 10 using the thin section analysis for quartz and is 2.0 in Wells DRB 11 and P12R. These values can be compared to that for an average sandstone of 5.8 (Pettijohn, 1957) or to an average arkose of 1.1. These parameters show that the source area was nearby and also had relatively high relief.

Further clues to the nearness of the source area can be obtained from the roundness of the sedimentary grains. The major portion of grains of Wells DRB 9 and DRB 10 are subangular and subrounded, and can be assigned a roundness value of 0.4, as determined by standard methods (Pettijohn, 1957). Published graphs (Pettijohn, 1957) that plot distance of transport against roundness of grains indicate that granodiorite pebbles of 0.4 degree of roundness have not traveled more than about 24 km from their source area. Based on the assumption that the schists and gneisses under SRP are no harder than a granodiorite, 24 km is also the approximately maximum distance of transport of the Triassic sediments found near the center of the Triassic basin. This approximate maximum distance indicates that the source was probably crystalline rock just northwest of the Triassic basin. Sources to the northeast or southwest were probably more than 24 km away, according to the outline of the Triassic basin inferred from aeromagnetic survey, and therefore are not likely sources for most of the sediments in Wells DRB 9, DRB 10, or DRB 11.

No fragments of material were found with density >2.73. Such material might have been supplied by a southeast source according to models constructed from gravity and magnetic surveys. Thus, sediments at Well DRB 10 probably did not come from the southeast.

Degree of sorting is another indicator of the source. Effectiveness of the sorting process depends mainly on the

density and viscosity of the transporting medium. Because of the abundance of large rock fragments in Well DRB 9 and their random orientation, some viscous medium must have transported them. One explanation would be a series of mudflows from the slopes of the source region.

Even though Well DRB 10 is located near the center of the Triassic basin, it contains the same mineral and rock fragment types as those found in Well DRB 9. This indicates that the sediments in the two wells came from regions of similar crystalline rock, and possibly from the same region. The degree of roundness of the particles in the two wells indicates that the source region was nearer than 24 km, which is consistent with a northwest source region supplying the sediments for both wells. Although a southwestward-flowing stream along the axis of the basin, bringing sediments from the northeast, cannot be ruled out, study of the sediments from Well DRB 10 does not support such a theory.

The Triassic rocks are apparently barren of microfossils and palynomorphs, as indicated by micropaleontological examination of 9 samples of both red and green material from DRB 10 and by palynological examination of 2 samples from DRB 9, 3 gray samples from DRB 10, and 1 gray sample from DRB 11.

Conceptual Triassic Basin Sedimentation

The selection of the location for Wells DRB 11 and P12R had two principal justifications. One was to explore a geophysically

inferred fault, and the other was to contribute to the understanding of the sedimentation in the Triassic basin; more specifically to answer the question of how the pebbly mudstone of Well DRB 9 related to the mudstones and sandstones of Well DRB 10. The sediments at Well DRB 11 are finer-grained, but more akin to the pebbly mudstones of Well DRB 9 than to the mudstones and sandstones of Well DRB 10. The sand, grit, and angular pebbles at Well DRB 11 are coarser than those at Well DRB 10, but not as plentiful. Coarse material from both the continuous core and as inferred from the electric log of Well DRB 11 is estimated to make up 10% of the sediments; whereas from the intermittent cores and the three-dimensional velocity log, 60% of Well DRB 10 is estimated to be sand. Wells DRB 9 and DRB 10 had the same source area for the sediments. The mineralogy of Well DRB 11 indicates it also had the same source area. The question then arises, how did a large amount of coarse sand reach the location of Well DRB 10, further toward the basin center, without being deposited in abundance at the location of Well DRB 11? The answer to this question further elucidates the pattern of sedimentation in this Triassic basin.

Fanglomerates, landslide debris, and mudrock flow deposits originated on the steep fault scarps and were emplaced near scarp bases. These deposits were penetrated by Well DRB 9, and they represent deposits from the scarp face not influenced by streams that had a drainage area in the mountains behind the scarp face.

Well DRB 11 penetrated the same type of sediments but further from scarp face, where coarse material was not as common.

Alluvial fan deposits occurred where streams, supported by a significant drainage basin in the Triassic highlands to the northwest, emptied into the Triassic basin. Near the fault scarp the apex of such alluvial fans would occupy only a small area (Fig. 9), but toward the valley center these alluvial fan sediments would occupy an increasingly large area until the coalescing alluvial fans would cover most of the valley bottom. Well DRB 10 penetrated these sediments.

Streams draining the metamorphic highlands dumped most of the very coarse debris close to the mountain front, but periodic increases in stream energy from either storm precipitation or renewed uplift carried coarse particles to the center of the basin. There, the shifting channels of the stream reworked the sands to provide occasional crossbedding. However, the debris supplied and transported to the center of the basin by the shifting streams far exceeded the streams' ability to sort the material and to create any laterally extensive bedding. Mud was supplied in large volume from both the scarp-face ephemeral drainage and from the larger streams. Much of this mud may have originated from the soil in the highlands, but much may have originated by the chemical weathering of the metamorphic minerals after they reached the valley. The mud deposits are characteritically massive and show no indication of bedding.

It is possible that there may have been a valley center longitudinal stream, but if so, the stream's energy was probably low compared to that of the streams draining the mountains. The valley center sediments, if they are represented by the rocks at Well DRB 10, are not well sorted. Occasionally mud-sand contacts in Well DRB 10 are nearly vertical with intricate crenulations indicating saturated sediments with low mechanical energy.

Water from the streams draining the Triassic mountains seeped downward into the alluvial sediments near the valley margin and upward near the valley center, thus concentrating salts by evaporation in the near surface soils of the valley center. The presence of caliche and calcium carbonate cement in the rocks near the valley center and the absence of these materials in rocks near the valley margin are evidence of this.

The sedimentary fill in the basin may have reached a maximum thickness of 1800 to 2400 m greater than at present; thus, the clayey sediments were compacted, reducing their permeability and porosity. Subsequent erosion (Jurassic - Early Cretaceous) has not only removed the Triassic highlands, but also 1800 to 2400 m of former valley fill. This erosional cycle reduced both mountains and valleys to a single very flat surface, now evidenced by the contact of the Coastal Plain sediments with the Triassic and crystalline rocks.

CONCLUSION

Seismic reflection surveys and gravity-magnetic surveys indicate that the Dunbarton Triassic basin may be wider than originally interpreted from the aeromagnetic map (Marine and Siple, 1974). However, until the density and magnetic properties of the crystalline metamorphic or igneous rock underlying the Triassic red beds are known, interpretation of the geophysical information will be speculative. A fault inferred within the Dunbarton basin from seismic data has been demonstrated to be spurious on the basis of information obtained from exploration wells. This inferred fault was caused by the presence or absence of a masking reflector within the Coastal Plain sediments that permits or obscures reflections from the top of the Triassic red beds. This masking reflector may be correlated with a soil zone in a gravelly-and-gritty sandy clay, that perhaps has been abruptly removed in places by later erosion due to stream channeling. Although only one inferred fault was explored by drilling, the results cast doubt on the validity of other faults inferred from the same type of data.

Even though displacement of the Triassic surface may not occur, interpretation of the gravity and magnetic data indicates faults separating blocks of Triassic rock of different thicknesses. Exploratory drilling was not performed to an extent sufficient to demonstrate major faults separating these inferred blocks. A minor fault was found at the expected location for the fault but did not

have the correct dip to be the one inferred from the gravity-magnetic information. Thus, the validity of the faults inferred from the gravity-magnetic information was neither confirmed nor denied by the exploratory wells.

Prior to the intrabasinal faulting, when the Triassic sediments were filling the basin, a mountainous highland existed to the northwest that was separated from the basin by a border fault similar to those in the Basin and Range province today. The metamorphic rock presently found beneath the Coastal Plain sediments in this region of Triassic highlands accounts for all of the lithologic types of fragmental rocks found in the Triassic rocks. Mudrock flow material moved from the mountain face in the interstream areas of the Triassic basin and these poorly-sorted deposits of mud and boulders are penetrated by Well DRB 9. Farther from the mountain face the same poorly-sorted sediments occur but without boulders or material generally coarser than granule size, and these deposits are penetrated by Well DRB 11. Streams that drain the mountainous region back from the face deposited alluvial fans that enlarged areally but decreased in grain size as distance from the mountains increased. These muddy sand deposits are penetrated by Well DRB 10. Based on the mineralogy of the sediments at Wells DRB 10 and DRB 11, subsequent erosion not only removed the Triassic highland, but also removed 1800 to 2400 meters of Triassic sediments.

REFERENCES CITED

Christl, R. J., 1964, Storage of radioactive wastes in basement rock beneath the Savannah River Plant: USAEC Report DP-844, E. I. du Pont de Nemours & Co., Savannah River Laboratory, Aiken, SC.

Marine, I. W., 1974, Geohydrology of the buried Triassic basin at the Savannah River Plant: Amer. Assn. Petroleum Geol. Bull., v. 58, no. 9, p. 1825-1837.

Marine, I. W. and Siple, G. E., 1974, Buried Triassic basin in the Central Savannah River area, South Carolina and Georgia: Geol. Soc. America Bull., v. 85, p. 311-320.

Perry, E. A., Jr. and Hower, J., 1972, Late-stage dehydration in deeply buried pelitic sediments: Am. Assoc. Petroleum Geologists Bull., v. 56, no. 10, p. 2017.

Pettijohn, F. J., 1957, Sedimentary rocks, 2nd ed., Harper & Row, New York.

Pettijohn, F. J., Potter, P. E., and Siever, R., 1972: Sand and Sandstone: Springer-Verlag, Berlin.

Petty, A. J., Petrafeso, F. A., and Moore, F. C., Jr., 1965, Aeromagnetic map of the Savannah River Plant area, South Carolina and Georgia: U. S. Geol. Survey Geophys. Inv. Map GP-489.

Randazzo, A. F., Swe, W., and Wheeler, W. H., 1970, A study of tectonic influence on Triassic sedimentation, the Wadesboro basin, Central Piedmont: Jour. Sed. Petrology, v. 40, no. 3, p. 998-1006.

TABLE 1. SEMIQUANTITATIVE MINERALOGY OF SAMPLES FROM WELL DRB 10 BY X-RAY DIFFRACTION FROM USGS, percent

Depth, m	Description	Quartz	Ortho-clase	Plagio-clase	Calcite	Laumon-tite	Clay Minerals: Kaoli-nite	Illite Mica	Montmo-rillonite	Chlorite	Mixed Layer	Total
341.5-342.1	Gray semiconsolidated fine sandy clay, some maroon patches. Tuscaloosa formation	57	3	0	0	0	28	3	1	0	2	94
350.3-351.0	Hard light gray sandy clay, not plastic. Tuscaloosa formation	32	10	3	0	0	15	24	4	2	0	90
356.0-358.8	Top of Triassic Rock											
360.9-361.3	Red siltstone, thin layers of green siltstone and clay	13	0	11	0	0	0	0	20	15	31	90
371.6-372.5	Reddish brown siltstone	18	4	15	0	0	6	12	3	3	21	82
375.5-376.3	Red siltstone	12	3	9	0	0	5	29	0	8	23	89
408.4-408.9	Pinkish white arkosic sandstone	53	6	21	0	4	0	10	0	0	0	94
458.0-458.5	Reddish-brown sandstone and siltstone	12	6	19	0	0	0	24	0	20	7	88
513.0-513.5	Brownish tan arkose with bands of claystone and coarse sandstone	25	6	27	0	0	0	18	4	20	0	100
579.7-580.1	Pink arkose	38	0	22	0	15	7	15	0	4	0	101
642.5-643.0	Red mudstone	18	5	23	0	0	0	8	0	14	18	86
696.0-696.5	Maroon mudstone	13	6	16	0	0	0	30	0	12	9	86
	gray sandstone	32	9	27	0	5	0	13	0	6	6	98
697.9-698.2	Pink arkose	30	0	21	0	17	5	21	0	3	6	98
699.3-699.7	Maroon mudstone	15	0	14	0	0	12	24	0	9	0	74
763.0-762.5	Gray arkose	10	0	34	46	2	1	4	0	0	0	92
819.2-819.6	Gray sandstone	13	7	13	0	1	2	20	0	9	18	83
	Pinkish tan sandstone	23	7	24	0	8	0	16	0	7	7	92
821.3-821.6	Tan and gray sandstone	18	0	22	0	6	0	18	0	11	21	96
881.6-882.1	Gray white arkose	37	0	34	0	19	4	7	0	2	2	105
939.6-940.0	Yellow and gray sandstone	27	0	36	0	20	3	11	0	3	9	109
944.2-944.6	Brown gray claystone and sandstone	23	5	25	3	0	0	11	0	11	13	91
1006.5-1007.0	Red claystone	20	2	27	12	0	11	12	0	1	6	91
1072.4-1073.0	Red claystone	17	5	21	3	0	1	11	0	23	0	81
1144.7-1145.1	Reddish gray sandstone	22	5	26	3	12	0	17	0	5	8	98
1219.8-1220.2	Gray sandstone	40	11	27	0	8	0	5	0	2	13	106
	pink arkose	18	8	17	0	0	0	21	0	10	9	83
1280.4-1280.8	Pink and gray sandstone	23	8	32	0	27	2	10	0	2	1	105

TABLE 2. MINERALOGY OF CORE SAMPLES FROM WELL DRB 10 BY THIN SECTION PETROGRAPHY (USGS), percent

Depth, m	Description	Quartz	Feldspar	Calcite[a]	Laumontite	Epidote	Chlorite	Muscovite or Sericite	Biotite or Hornblende	Opaque Minerals	Ferruginous Cement or Matrix	Remarks
381.6-	Fine sandstone (Top)	30	5	0		2	2				60	Quartz as angular grains
376.3	Red sandy claystone (Middle)	15		0.3		5		tr			80	Quartz strained and cracked
408.4- 408.9	Pink arkosic sandstone	50	35	0	10	tr	tr	tr				Magnetite <5%, zeolites as cement; feldspar altered; quartz strained and cracked
458.0- 458.5	Maroon mudstone	∿5	∿5	0		∿5		∿5			80	
513.0- 513.5	Tan arkosic sandstone	45	20	0	25	<5	<5	<5		<5		Garnet tr; zeolites as cement; feldspar smashed; quartz mild strain, smashed
579.7- 580.1	Pink arkosic sandstone	50	25	0.7	15	<5	tr	tr		<5		Clots of quartz, chlorite, and epidote replace sites of mafic minerals. Quartz strained.
642.5- 643.0	Red mudstone	25		0		<5		<5			70	
696.0-	Maroon mudstone (Top)	40				10	∿10				40	
696.5	Gray sandstone (Bottom)	60	18	0	10	5	<5					Magnetite <5
697.9- 698.1	Pink arkosic sandstone	50	10	0	20	5	5	<5	tr	5		Clots of chlorite and epidote replace site of mafic minerals
699.2- 699.7	Maroon mudstone	50	<5	0		<5		<5			<50	
762.0-	Limy sandstone (Top)	60	30	25.7		<5						
762.5	Pink arkosic sandstone (Middle)	40	35	2.3	10	<5	<5	<5				Quartz crushed and granulated
819.2	Tan sandstone (Top)	35	15	0		<5		<5		5-10		Dirty chlorite rich matrix 50%, quartz strained and crushed
819.6	Pink arkosic sandstone (Bottom)	60	20	0	5	<5				5		
821.2- 821.6	Tan and gray sandstone	40	25	0	15	5	5			<5		Amorphous matrix 10%, zoisite tr; chlorite and magnetite replaces biotite; quartz strained
881.6- 882.1	Gray arkosic sandstone	40	15	0	30	5	<5			<5		
939.6-	Yellow and gray sandstone (Top)	40	25	0	25	tr				<5		Clay 5-10%
940.0	(Middle)	35	15	0	5	5	<5	30		5	5	
944.2- 944.6	Gray claystone and sandstone	35	<5	1.7		<5		10		<5	50	

TABLE 2. (Continued)

Depth, m	Description	Quartz	Feldspar	Calcite[a]	Laumontite	Epidote	Chlorite	Muscovite or Sericite	Biotite or Hornblende	Opaque Minerals	Ferruginous Cement or Matrix	Remarks
1006.5-1007.0	Red claystone	20	10	14.7		10		10			50	Calcite nodules
1072.4-1073.0	Red claystone	35	tr	2.0		5		5			40	Calcite nodules
1144.7-1145.1	Reddish gray sandstone	45	15	0.7	10	10	5	5		5		Apatite tr
1219.8-1220.2	Pink arkosic sandstone (Top)	40	15	0	25	<5	<5	<5		5		
	Gray sandstone (Bottom)	50	10	0	<5	<5	<5	10		5		
1280.4-1280.8	Pink and gray sandstone	35	20	0	30	<5	<5	5		5		

a. By carbonate analysis.

TABLE 3. MINERALOGY OF CORE SAMPLES FROM WELL DRB 11 BY X-RAY DIFFRACTION, percent

Depth, m	Description	Quartz	Orthoclase	Plagioclase	Calcite	Hematite	Clay Minerals				
							Kaolinite	Illite or Mica	Chlorite	Montmorillonite	Mixed Layer
311.5	Light gray sandy clay	81	5				13	1			
317.7	Gray hard medium sand	85	12				3				
321.3	Greenish gray siltstone	89	3				7	1			
326.1	Red and gray siltstone	97					3				
	TOP OF TRIASSIC										
326.8	Red siltstone	42		4		52	2				
326.8	White siltstone	78		6			16				
332.4	Red mudstone (swelled)	65		27		3	4	1			
335.2	Red mudstone (swelled)	66		18		6		5	5		tr
340.6	Green clay seam[a]	51		11		2		6	6		
342.2	Green clay	57	2	31		tr		3	7		
349.1	Maroon mudstone	76	1	20		1			1		tr
354.8	Gray clay seam	31	1	7	57	1		1	2		
363.7	Maroon mudstone	56	tr	24	tr	9		4	5		
370.4	Green seam	73	2	22		1		1	1		
379.9	Gritty mudstone adjacent to 70° shear	63	tr	31	tr	2			1		
384.5	Maroon mudstone	56	tr	24	tr	4		10	4		
389.8	Maroon mudstone from waxy face of 70° shear	68	3	22		3		3	2		tr
396.3	Maroon mudstone with green dots	58	tr	27		4		8	3		
397.0	Maroon mudstone	46	tr	12		16		13	11		
411.8	Maroon mudstone with very fine sand	54	2	35		3		4	1		1
443.7	Maroon mudstone	56	3	28		5		6	2		tr
457.4	Maroon mudstone	53	tr	32		tr		9	4		
480.2	Maroon mudstone	58	tr	26		5		6	4		
503.8	Maroon mudstone	50	4	32		7		3	4		
505.9	Purple mudstone	61	1	31		tr		2	4		
533.2	Maroon mudstone	60		34		3		1	2		
564.2	Maroon mudstone	48		44		3		2	3		
579.2	Maroon mudstone with medium sand	67	5	26		1		1	tr		

TABLE 3. (Continued)

Depth, m	Description	Quartz	Orthoclase	Plagioclase	Calcite	Hematite	Clay Minerals				
							Kaolinite	Illite or Mica	Chlorite	Montmorillonite	Mixed Layer
580.4	Maroon mudstone from eroded core	48		33		4		12	3		
587.8	Green plastic clay seam 1 inch thick	53	2	27	1	1		10	6		
610.8	Maroon mudstone with calcite dots	41	2	19	29	4		3	2	tr	tr
713.7	Maroon mudstone from "caving zone"	66	5	21		2		2	3		tr
714.2	Maroon mudstone from below "caving zone"	65		27		3		2	3		
	"caved material" from bottom of hole	53	2	22		6		11	5		
730.2	Maroon mudstone (eroded core)	53	1	27		5		8	4		
744.8	Maroon mudstone from zone of cone fractures	56		30		6		1	5		tr
763.1	Maroon mudstone	59	4	22		6		4	5		tr
793.1	Maroon mudstone	53	4	27		3		6	7		
823.1	Maroon mudstone	65		26		3		3	4		
853.8	Maroon mudstone	60	1	35		4		2	2		
884.0	Maroon sandy mudstone	44		30	20	3		1	2		tr
888.6	Calcite nodules in maroon mudstone	10	1	4	82	1		1	1		
914.3	Maroon mudstone	62		26	1	3		2	6		
944.9	Maroon sandy mudstone with calcite nodules	61	3	29	2	2		2	1		
975.6	Maroon mudstone	52		29	tr	4		10	5		
986.9	Maroon mudstone above sheared zone	54		35		4		3	4		
990.4	Maroon mudstone within sheared zone	63		22		5		6	4		
991.6	Gouge material at bottom of sheared zone	52	8	27	tr	10			3		
993.6	Maroon mudstone below sheared zone	27	5	14	45	3		1	5		
1011.9	Maroon mudstone	59		29		5		3	4		

a. Contains 25% unknown

TABLE 4. RELATIVE PERCENTAGES OF MINERALS IN SAMPLES[a] FROM WELL DRB 11

Sample	Depth, m	Mixed Layer[b]	Illite	Chlorite	Halloysite	Hematite
1	331.9	81	10	0	4	5
2	404.2	81	13	0	0	6
3	480.7	72	15	5	0	8
4	558.7	68	24	0	0	8
5	631.6	37	25	20	0	18

a. <2 microns.
b. Illute/montmorillonite material

TABLE 5. MINERALOGY OF SAMPLES FROM WELL P12R BY X-RAY DIFFRACTION, percent

Depth, m	Description	Quartz	Ortho-clase	Plagio-clase	Laumon-tite	Hematite	Clay Minerals[a]			
							Kaolinite	Illite or Mica	Chlorite	Mixed Layer
302.4	White clay	88	9				3	tr		
315.8	White friable sand	87	9				3	1		
324.4	Red friable sand	73	20				5	2		
331.3	White friable coarse sand	88	3	1			8			
331.6	Top of Triassic rocks									
332.1[b]	Soft tan mudstone	61		tr			31			
332.3	Soft red mudstone	70		1		12	17	tr		
339.1	Soft red mudstone	59		39				7		tr
340.7	Hard red mudstone (cracked when dried)	59	1	23		8	3	6		tr
344.9	Hard red mudstone (cracked)	51		32		9	4	tr	4	tr
345.0	Green inclusion of red mudstone	58	2	36				1	3	tr
351.7	Red mudstone	60	2	30	tr	4		3	1	tr
351.8	Green mudstone	62	2	35				1	tr	tr
352.6	Hard red mudstone (cracked)	59	1	33		4		2	1	tr
353.5	Green clay	60	4	32	tr			3	1	tr
354.0	Hard green and red mudstone	59	2	36		2		1		tr
357.2	Hard red mudstone (cracked)	59	3	28		6		3	1	
361.2	Hard red mudstone (cracked)	57	1	32		4		4	2	tr
371.0	Hard pebbly mudstone	72	2	22	tr	2		tr		1
376.7	Hard green clay	53	2	42				2	1	
378.7	Hard green and red mudstone	57	1	33		4		4	1	tr
380.6	Pebbly mudstone	54	2	39		3		1	1	tr
Average of sand above Triassic		84.0	10.25	0.25	0	0	5.25	0.9	0	0
Average of Triassic		59.4	1.5	29.0	0	3.4	3.2	2.0	1.0	0.5

a. Montmorillonite could not be identified with X-ray machine used.
b. Observed X-ray peaks indicate 8% phosgenite ($PbCO_3 \cdot PbCl_2$), however this identification is suspected to be erroneous.

TABLE 6. AVERAGE MINERAL COMPOSITION OF TRIASSIC ROCK, percent

Well	Description	Quartz	Orthoclase	Plagioclase	Hematite	Clay Minerals				
						Kaolinite	Illite or Mica	Chlorite	Montmorillonite	Mixed Layer
DRB 10	Pink friable sandstone	27.6	5.1	26.0			12.7	6.3		5.0
	Grayish brown hard sandstone	16	3.4	19.4			22.6	11.4		9
	Maroon mudstone	19	3.6	19.5			14.4	8.0		15
	Maroon mudstone[a]	42	17							
DRB 11	Maroon mudstone	55.4	1.1	24.7	3.8		3.9	3.6		
P12R	Maroon mudstone	59.4	1.5	29.0	3.4		2.0	1.0		0.5

a. By thin section petrography.

TABLE 7. FRAGMENTS IN TRIASSIC ROCK IN WELL DRB 9, percent of total fragments

Depth, m	Biotite-Hornblende-Chlorite Schists and Associated Gneisses	Quartzite	Augen-Gneiss
318.2-323.1	10	10	80
324.3-326.1	10	10	80
327.7-328.9	10	40	50
328.9-330.7	30	70	0
330.7-332.2	10	90	0
332.2-335.0	20	80	0
336.2-339.6	60	40	0
339.6-340.8	45	30	25
340.8-346.0	20	40	40
346.0-349.9	50	50	0
349.9-352.4	60	40	0
352.4-353.3	75	25	0
353.6-357.5	50	40	10
357.5-361.2	40	40	20
387.1-396.5	20	0	80
420.6-427.6	10	0	90
621.8-626.4	5	0	95
805.3	0	0	100

TABLE 8. FRAGMENTS IN TRIASSIC ROCK IN WELL DRB 10, percent of total fragments

Depth, m	Chlorite Schists and Associated Gneiss	Quartzite	Augen-Gneiss
358.7- 364.5	80	20	0
364.5- 366.4	95	5	0
366.4- 373.1	60	40	0[a]
373.1- 376.4	70	30	0
376.4- 381.0	80	20	0
406.3- 409.6	70	30	0[a]
455.1- 458.4	80	20	0[a]
577.6- 581.0	60	40	0
640.1- 645.6	60	40	0
645.6- 647.1	70	30	0
695.6- 696.8	30	70	0[a]
697.4- 702.9	50	50	0
760.8- 768.1	30	70	0
816.9- 823.0	40	60	0[a]
880.9- 883.6	70	30	0
937.6- 940.6	70	30	0
940.6- 944.9	50	50	0
1002.5-1009.2	40	60	0
1066.5-1072.9	50	50	0
1140.3-1147.0	70	30	0
1214.3-1220.4	70	30	0[a]
1277.1-1283.8	80	20	0[a]

a. Some augen-gneiss may be present due to increased K-feldspar content in the rocks, but no augen-gneiss rock fragments were found.

LIST OF FIGURES

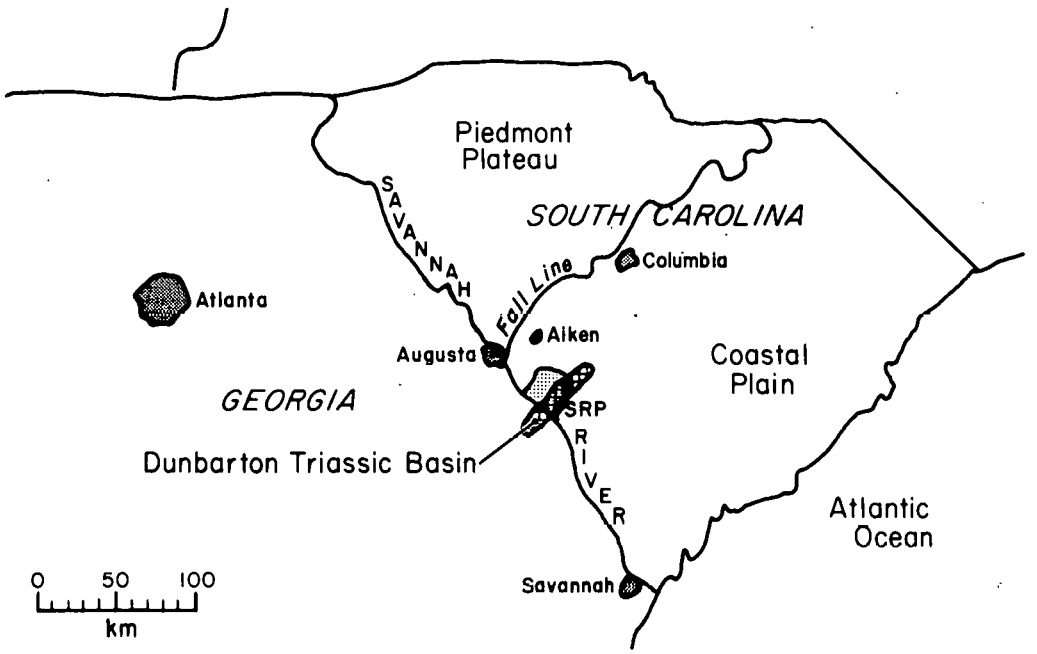

Figure 1. Location of the Dunbarton basin.

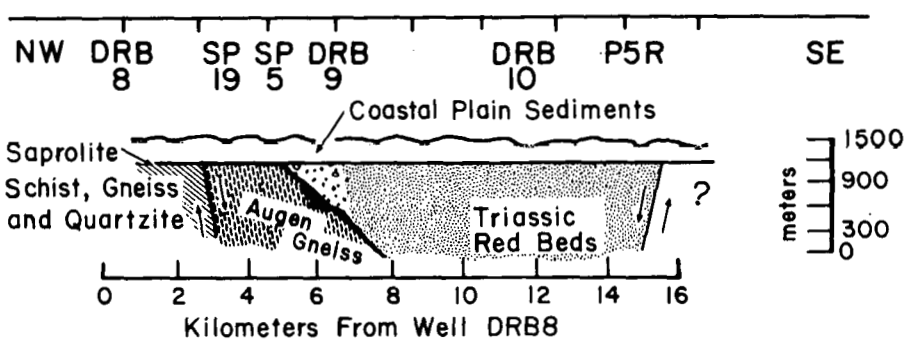

Figure 2. Conceptual cross section of the Dunbarton Triassic basin according to Marine and Siple (1974). DRB 8, 9, 10, and P5R are wells; SP5 and 19 are shot points on seismic traverse.

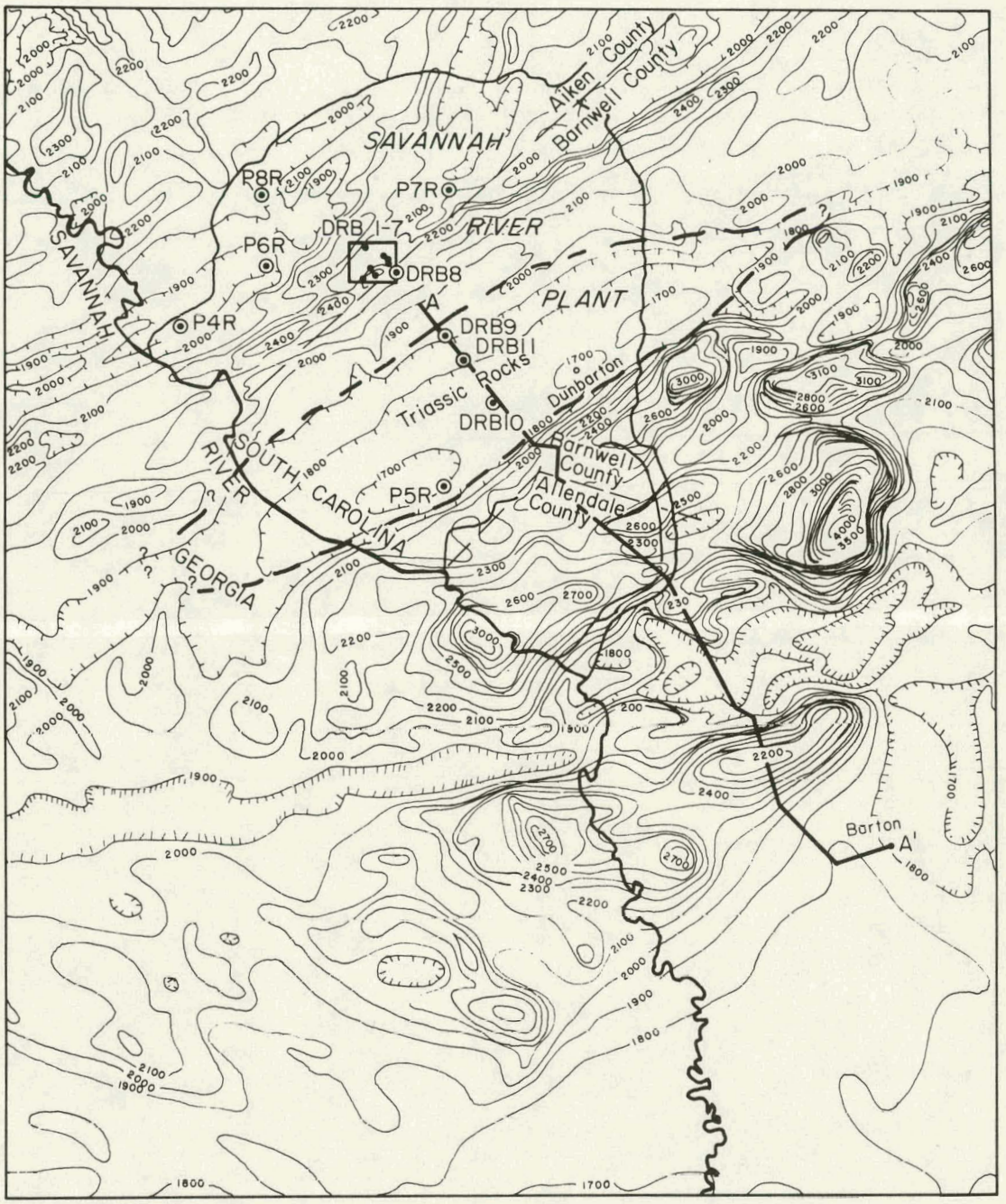

Figure 3. Aeromagnetic map showing the Dunbarton Triassic basin according to Marine and Siple (1974) and the ground magnetic traverse to Barton, SC. Note the aeromagnetic characteristics of the region of explored crystalline metamorphic rock in the northwestern part of SRP, the Triassic basin in the southeastern part, the region of magnetic highs and lows southeast of SRP, and the featureless region around the south of Barton, SC. (Aeromagnetic contours are taken from Petty, Petrafeso, and Moore, 1965.)

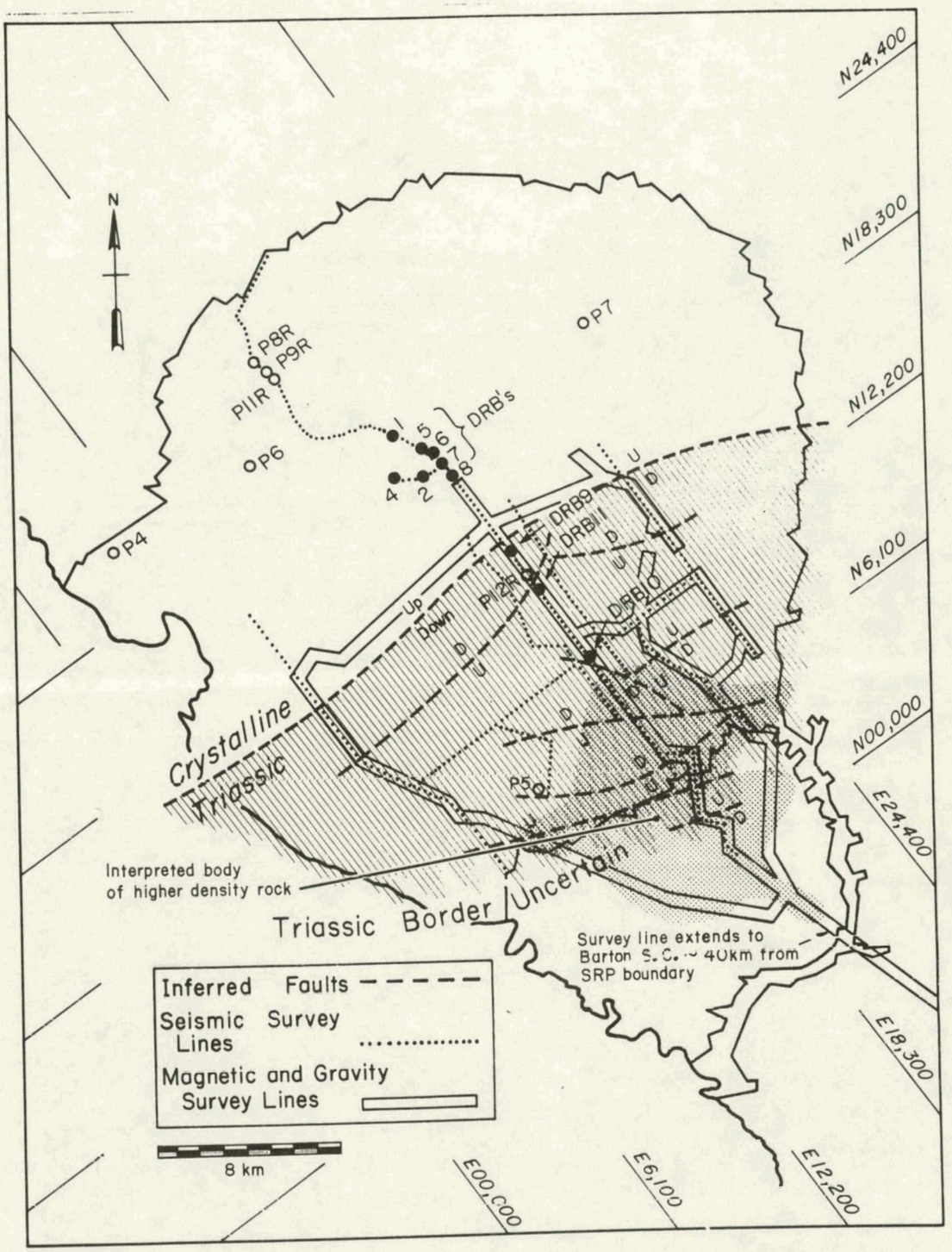

Figure 4. Locations of wells, reflection seismic traverses, the Dunbarton Triassic basin as presently inferred, faults in the Triassic basin from the seismic survey, and inferred body of denser metamorphic or igneous rock underlying the Triassic rock. Coordinates are from an arbitrary grid used at SRP in meters.

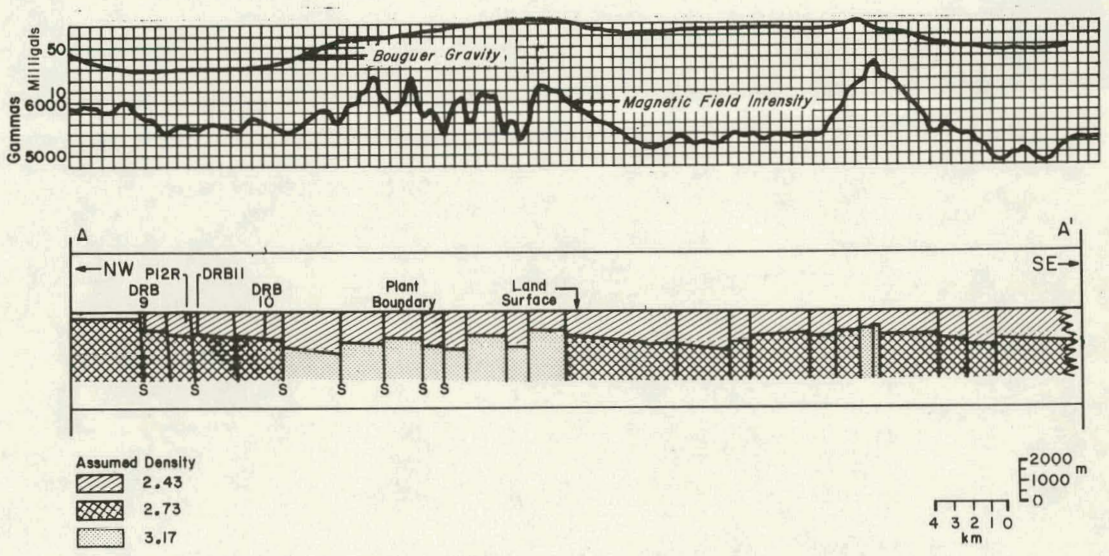

Figure 5. Cross-sectional model of Dunbarton Triassic basin based on gravity-magnetic traverse along A-A' of Fig. 3.

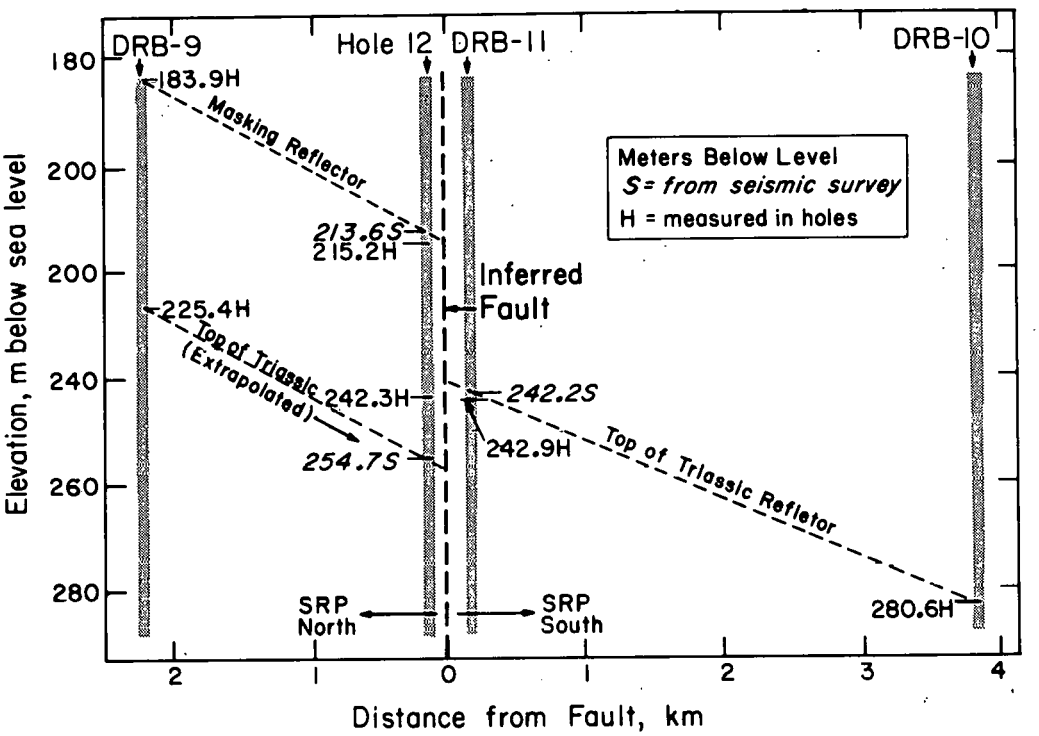

Figure 6. Correlation of seismic and drill hole information in the vicinity of an inferred fault.

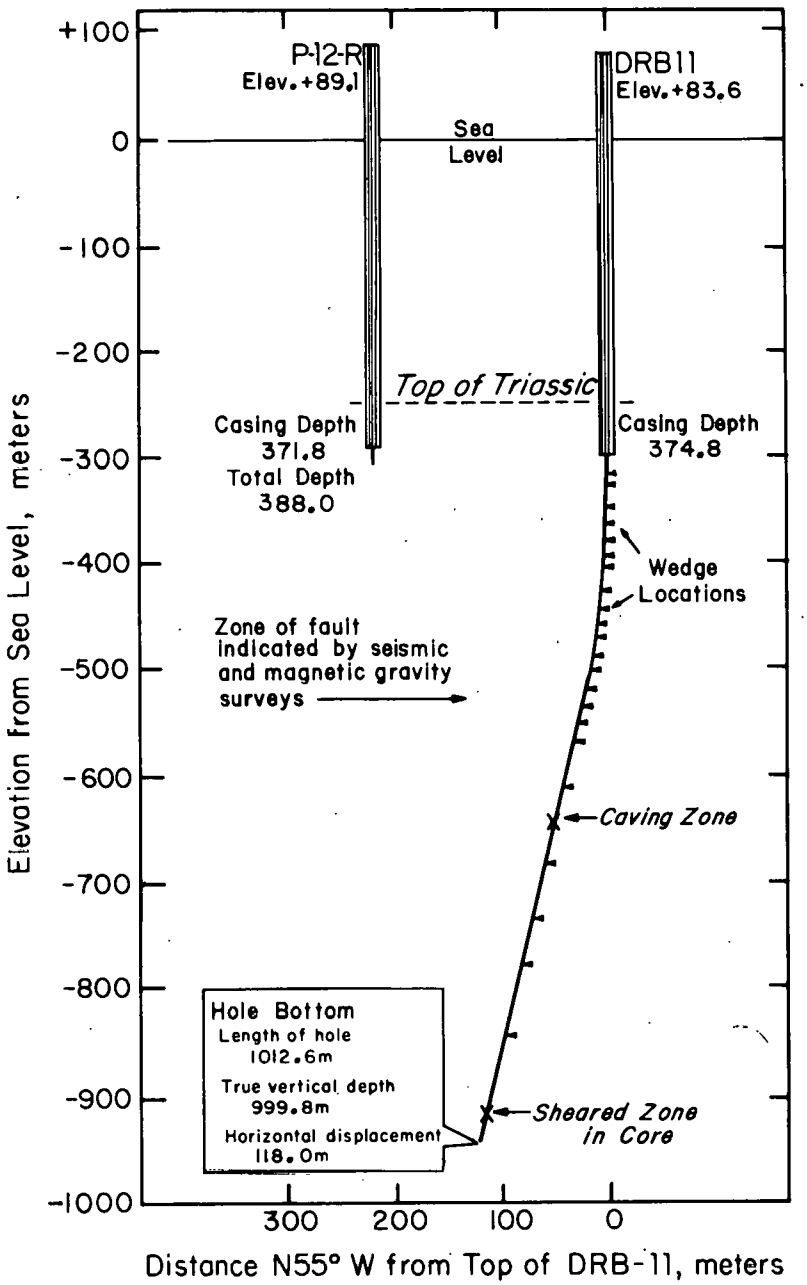

Figure 7. Profile of Wells DRB 11 and P12R and inferred fault zone.

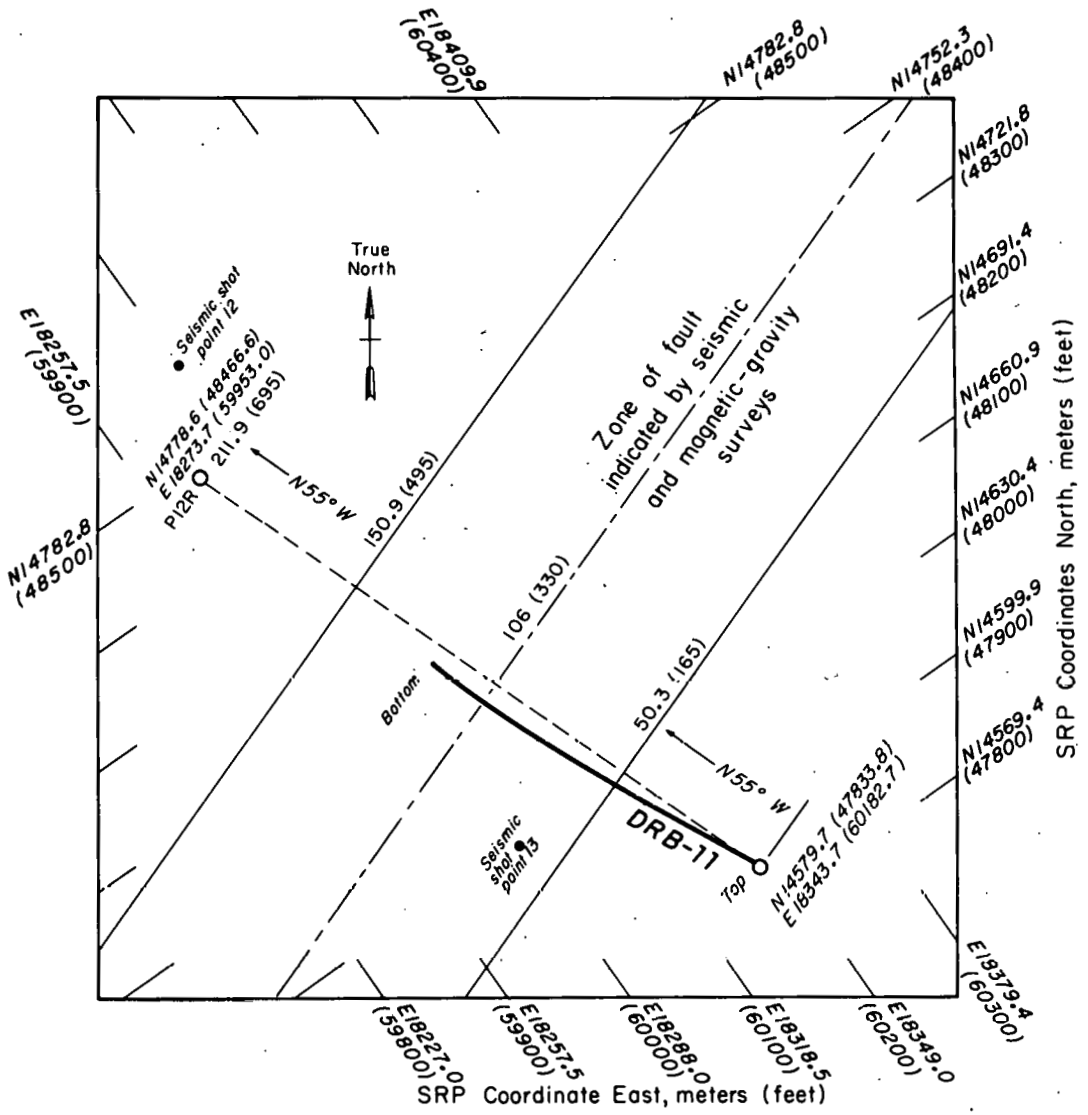

Figure 8. Locations of Wells DRB 11 and P12R and inferred fault zone.

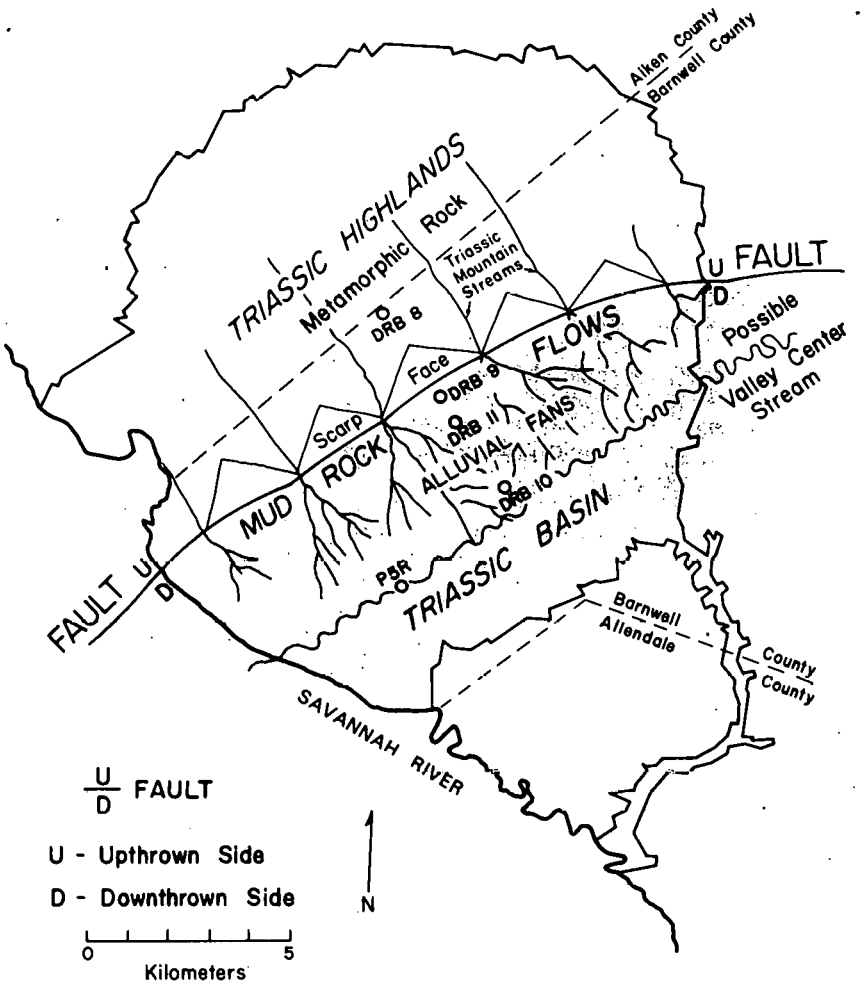

Figure 9. Schematic diagrams of land forms of the Dunbarton Triassic basin in late Triassic time.